www.cb.wiley.com

# Isospongian Diterpenoids from the Leaves of *Amomum* tsao-ko Promote GLP-1 Secretion via Ca<sup>2+</sup>/CaMKII and PKA Pathways and Inhibit DPP-4 Enzyme

Yun Wang,<sup>[a, b]</sup> Sheng-Li Wu,<sup>[b, c]</sup> Xin-Yu Li,<sup>[b, c]</sup> Pianchou Gongpan,<sup>[b]</sup> Hang Fu,<sup>[a, b]</sup> Xiang-Ming Liao,<sup>[b, c]</sup> Yi Yang,<sup>[d]</sup> Mei Huang,<sup>[d]</sup> Xiao-Yan Huang,<sup>[b]</sup> Yun-Bao Ma,<sup>[b]</sup> Da-Hong Li,<sup>[a]</sup> and Chang-An Geng\*<sup>[b, c]</sup>

Three uncommon isospongian diterpenoids including a new one, 3-epi-kravanhin A (2), were isolated from the leaves of Amomum tsao-ko. Compounds 2 and 3 dose-dependently promoted GLP-1 secretion on STC-1 cells with promotion ratios of 109.7% and 186.1% (60  $\mu$ M). Mechanism study demonstrated that the GLP-1 stimulative effects of 2 and 3 were closely related with Ca²+/CaMKII and PKA pathways, but irrelevant to GPBAR1 and GPR119 receptors. Moreover, compound 1 showed DPP-4 inhibitory activity with an IC50 value of 311.0  $\mu$ M.

Molecular docking verified the binding affinity of 1 with DPP-4 by hydrogen bonds between the  $\gamma$ -lactone carbonyl (C-15) and Arg61 residue. Bioinformatics study indicated that compound 1 exerted antidiabetic effects by improving inflammation, oxidative stress and insulin resistance. This study first disclosed the presence of isospongian diterpenoids in *A. tsao-ko*, which showed antidiabetic potency by promoting GLP-1 secretion and inhibiting DPP-4 activity.

# Introduction

Isospongian diterpenoids are an unusual class of compounds with a tetracyclic 6/6/6/5 framework, which are initially isolated from marine organisms such as sponges and nudibranchs. [1-3] Different from the spongian skeleton that features a 3,4-fused tetrahydrofuran, isospongian diterpenoids contain a 2,3-fused tetrahydrofuran in the structure. [4] In 1985, Gustafson *et al* reported the first isospongian diterpenoid, marginatafuran, from *Cadlina luteomarginata*, whose structure was resolved by X-ray diffraction analysis. [5] After that several isospongian diterpenoids were further isolated from different marine organisms, *eg. Aplysilla polyrhaphis, Aplysilla glacialis* and *Cadlina luteomarginata*. [4,6,7] Isospongian diterpenoids exhibited a wide range of biological activities, including anti-tumor, anti-inflammatory, antiviral, antifungal and antihypertensive effects,

capturing the interests of pharmacists and organic chemists. [8–11] Besides the marine organisms, isospongian diterpenoids were sporadically discovered in terrestrial Amomum plants. In 2013, Yin et~al reported four isospongian diterpenoids, kravanhins A–D, from the fruits of Amomum~kravanh, showing NO inhibitory effects on LPS-activated RAW264.7 cells. [9] In 2022, Ding et~al reported the first isospongian diterpenoid glycoside, kravanhin A 3-O- $\beta$ -D-glucopyranoside, from the fruits of Amomum~villosum with GLP-1 promoting activity. [12] Structurally, the isospongian diterpenoids from Amomum~plants~always~maintain~a~8,9-cis-fused skeleton, different from the 8,9-trans fusion in the marine sources. From a biosynthetic point of view, isospongian diterpenoids in Amomum~plants~were~proposed~to~be~derived~from~the~common~labdane~diterpenoids~by~the~condensation~of~C-8~and~C-16~positions.

Diabetes mellitus (DM) is a chronic condition characterized by high blood sugar levels, which results from inadequate insulin secretion or reduced response to insulin.[13-15] The International Diabetes Federation (IDF) estimated that about 537 million adults are living with diabetes in 2022, and this number will rise to 643 million by 2030.[16] Type 2 diabetes mellitus (T2DM) occupying more than 90% of the cases is the most common type of DM.[17] Although the pathogenesis of T2DM is not fully clarified, the involvement of genetic, environmental and lifestyle factors are widely accepted. [18] Untreated or poorly controlled DM can lead to various acute and chronic complications such as cardiovascular disease, neuropathy, retinopathy, nephropathy and foot ulcers, which significantly impact the quality of life and longevity of the patients.[19,20] Presently, many kinds of antidiabetic drugs are available on the market, whereas they are still unsatisfied due to the inevitable side-effects and high risks of hypoglycemia. Hence, it is required

- [b] Y. Wang, S.-L. Wu, X.-Y. Li, P. Gongpan, H. Fu, X.-M. Liao, X.-Y. Huang, Y.-B. Ma, C.-A. Geng Key Laboratory of Phytochemistry and Natural Medicines, Kunming Institute of Botany, Chinese Academy of Sciences, Kunming 650201, People's Republic of China E-mail: gengchangan@mail.kib.ac.cn
- [c] S.-L. Wu, X.-Y. Li, X.-M. Liao, C.-A. Geng University of Chinese Academy of Sciences, Beijing 100049, People's Republic of China
- [d] Y. Yang, M. Huang Nujiang Green Spice Industry Research Institute, Lushui, Yunnan 673100, People's Republic of China
- Supporting information for this article is available on the WWW under https://doi.org/10.1002/cbdv.202401407

<sup>[</sup>a] Y. Wang, H. Fu, D.-H. Li Key Laboratory of Structure-Based Drug Design & Discovery, Ministry of Education, and School of Traditional Chinese Materia Medica, Shenyang Pharmaceutical University, Shenyang 110016, People's Republic of China

to explore novel hypoglycemic candidates with different mechanism and target.

Tsaoko Fructus, known as Caoguo in China, is the dried mature fruits of Amomum tsao-ko Crevost et Lemaire (Zingiberaceae), which has been documented in every edition of Chinese Pharmacopoeia.<sup>[21]</sup> Amomum tsao-ko is mainly cultivated in Yunnan, Guangxi and Guizhou provinces of China, of which Yunnan is the main planting area occupying 90% of the production. In the traditional Chinese medicine (TCM) system, Tsaoko Fructus has the effects of drying dampness, warming the middle, expelling malarial parasites and resolving phlegm, and is commonly used for treating malaria and gastrointestinal diseases.[22-24] The chemical constituents in A. tsao-ko mainly include diphenylheptanes, sesquiterpenes, monoterpenes, flavonoids and phenols, [25-29] which show antibiotic, anti-tumor, anti-cancer, anti-inflammatory, anti-diabetic and neuroprotective effects.[30-32] Yu et al disclosed that the methanol extract of A. tsao-ko showed hypoglycemic and antioxidant effects in vivo, whereas the antidiabetic constituents remain unclear.[33]

Our group is committed to search versatile antidiabetic candidates from natural sources. [34-41] Previous study on the fruits of A. tsao-ko yielded a series of flavonoids, diarylheptanoids, monoterpenes and hydroxytetradecenals showing  $\alpha$ -glucosidase, PTP1B and Gpa inhibitory activity. [42-45] Whereas the antidiabetic effect of different parts other than fruits of A. tsao-ko is still unclear, especially the leaves and stems that occupy most of the biomass. As a continuous study to reveal the antidiabetic effects and constituents of A. tsao-ko, three isospongian diterpenoids including a new one (Figure 1) were isolated from the leaves of this plant. Herein, we report their isolation, structural elucidation, and antidiabetic efficacy by stimulating GLP-1 secretion and inhibiting DPP-4 enzyme.

# **Results and Discussion**

# **Structure Identification**

Compound **2** possessed a molecular formula of  $C_{20}H_{28}O_4$  as deduced from the  $[M+Na]^+$  ion at m/z 355.1880 (calcd. for 355.1880, 0.0 mDa) in positive HRESIMS. The IR absorptions at 1738 and 1642 cm<sup>-1</sup> and UV absorption at 217 nm indicated the presence of an  $\alpha$ , $\beta$ -unsaturated  $\gamma$ -lactone in the structure. The  $^1$ H-NMR spectrum displayed four methyl singlets at  $\delta_H$  0.78 (3H), 0.90 (3H), 0.91 (3H) and 1.01 (3H), two oxygen-containing methines at  $\delta_H$  3.48 (t, J=2.7 Hz) and 5.30 (br s), and a trisubstituted double bond at  $\delta_H$  5.80 (d, J=2.0 Hz). By analyzing the  $^{13}$ C NMR and HSQC spectra, 20 carbons including four sp $^3$  methyls, five sp $^3$  methylenes, four sp $^3$  and one sp $^2$  methines,

Figure 1. The structures of compounds 1–3.

and three sp³ and three sp² quaternary carbons were recognized (Table 1). Besides the above mentioned two carbonyls ( $\delta_{\rm C}$  213.6 and 174.2) and a pair of double bond ( $\delta_{\rm C}$  170.3 and 115.5), four rings were required to fulfill the unsaturation. Its ¹H and ¹³C NMR data showed high similarity with kravanhin A (3), except for the chemical shifts at C-3 position ( $\delta_{\rm H}$  3.48 in **2** vs 3.32 in **3**;  $\delta_{\rm C}$  74.9 in **2** vs 78.5 in **3**), indicating the variation nearby. Different with kravanhin A, the coupling split of H-3 in **2** was *t*-like (J=2.7 Hz) suggesting the equatorial orientation of H-3, and thus H-3 was  $\beta$  oriented. This deduction was well confirmed by the correlation of H-3 with Me-19 in the ROESY spectrum.

In the  $^1\text{H-}^1\text{H}$  COSY spectrum, the correlations of  $\text{H}_2-1/\text{H}_2-2/$  H-3, H-5/H<sub>2</sub>-6, and H-9/H<sub>2</sub>-11/H<sub>2</sub>-12, in combination with the HMBC correlations from H<sub>3</sub>-18(19) to C-3 and C-5, from H<sub>3</sub>-20 to C-1, C-5 and C-9, from H<sub>3</sub>-17 to C-7, C-9 and C-16, from H-16 to C-7, C-9, C-12, C-14 and C-15 verified the isospongian diterpenoid skeleton. In the ROESY spectrum, the correlations of H-3/H<sub>3</sub>-19, H-5/H-9, H-5/H<sub>3</sub>-17, H-16/H<sub>3</sub>-20 verified the  $\alpha$ -orientation of OH-3, H-5, H-9 and Me-8 (C-17), and  $\beta$ -orientation of Me-10 (C-20) and H-16 (Figure 2). Its absolute configuration was determined to be identical with kravanhin A from the

<b>Table 1.</b> $^{1}\text{H}$ and $^{13}\text{C}$ NMR Data of <b>2</b> in CDCl <sub>3</sub> ( $\delta$ in ppm, $J$ in Hz). $^{[a]}$		
No.	$\delta_{H}$	$\delta_C$
1	1.58 dt (12.4, 3.7)	33.5, CH <sub>2</sub>
	1.46 dt (12.4, 3.2)	
2	1.83 m	25.3, CH <sub>2</sub>
	1.55 m	
3	3.48 t (2.7)	74.9, CH
4	-	38.0, C
5	2.36 dd (12.5, 7.5)	42.2, CH
6	2.52 dd (17.5, 7.5)	35.9, CH <sub>2</sub>
	2.35 dd (17.5, 12.5)	
7	-	213.6, C
8	-	50.1, C
9	1.62 dd (11.8, 3.6)	59.9, CH
10	-	38.0, C
11	1.68 m	19.1, CH <sub>2</sub>
	1.56 m	
12	2.86 ddt (19.5, 5.2, 2.4)	25.0, CH <sub>2</sub>
	2.48 m	
13	-	170.3, C
14	5.80 d (2.4)	115.5, CH
15	-	174.2, C
16	5.30 br s	81.6, CH
17	1.01 s	20.3, CH <sub>3</sub>
18	0.91 s	27.8, CH <sub>3</sub>
19	0.90 s	22.2, CH <sub>3</sub>
20	0.78 s	15.5, CH₃

[a]  $^{1}$ H-NMR data were measured at 600 MHz,  $^{13}$ C NMR data were measured at 150 MHz.



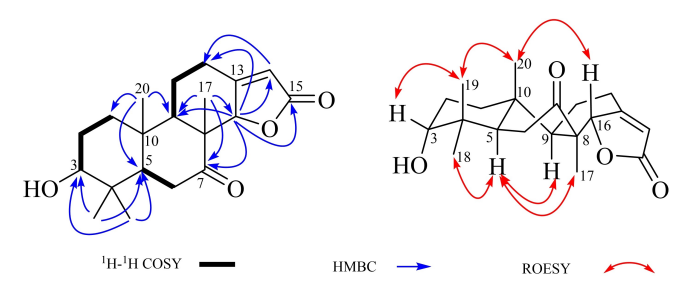


Figure 2. Key <sup>1</sup>H-<sup>1</sup>H COSY, HMBC and ROESY correlations of 2.

negative optical rotation ( $[a]_{\rm D}^{23}$  –175.2, MeOH) and negative cotton effect at 228 (–17.03) nm in ECD spectrum. Thus, the structure of **2** was determined to be 3-*epi*-kravanhin A.

Two known isospongian diterpenoids were identified as kravanhin C (1) and kravanhin A (3) by comparing their spectroscopic data with those reported in the literature. [9]

#### **GLP-1 Promotion**

Considering that isospongian diterpenoids were first isolated from *A. tsao-ko*, compounds **1–3** were assayed for their antidiabetic potency by stimulating GLP-1 secretion in STC-1 cells. As shown in Table 2, compounds **2** and **3** could significantly promote GLP-1 secretion by 109.7% and 186.1% at 60  $\mu$ M. Their dose-effect relationships were further studied at concentrations of 5–160  $\mu$ M (Figure 3), and compounds **2** and **3** could dose-dependently promote the secretion of GLP-1 without influencing the cell viability.

**Table 2.** Promoting effects of **1–3** on GLP-1 secretion in STC-1 cells (60  $\mu\text{M}).^{\text{[a]}}$ 

• •			
No.	GLP-1 content (pg/mL)	(pg/mL) Promoting rate (%) <sup>[b]</sup>	
1	25.3 ± 49.7	/ <sup>[c]</sup>	
2	$149.3 \pm 24.6$	109.7 ± 34.6	
3	$203.6 \pm 10.9$	186.1 ± 15.3	
Cholic acid <sup>[d]</sup>	$127.8 \pm 25.6$	79.6 ± 36.0	

[a] Data were expressed as mean  $\pm$  SDs (n=3). [b] Promotion rates were denoted as the increased percentage of GLP-1 contents vs control group. [c] No promoting effect was obtained. [d] Cholic acid was used as the positive control.

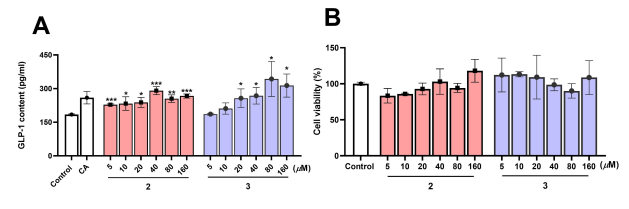
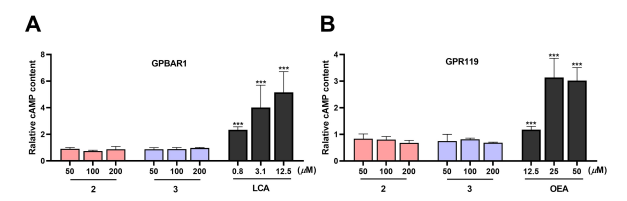


Figure 3. Dose-effect relationships of 2 and 3 on GLP-1 secretion (A) and cell viability (B). Cholic acid (CA) was used as the positive control. \*P < 0.05, \*\*P < 0.01, \*\*\*P < 0.001 vs control. Data were expressed as mean  $\pm$  SDs (n = 3).

# **Mechanism Study**

G protein-coupled receptors (GPCRs) that were highly expressed on intestinal endocrine cells were closely related with GLP-1 secretion. [46,47] To testify the possible targets of compounds **2** and **3** in stimulating GLP-1, their effects on two GPCRs, GPBAR1 and GPR119, were further evaluated. As shown Figure 4, compounds **2** and **3** was inactive to both GPBAR1 and GPR119 receptors at concentrations of 50, 100 and 200  $\mu$ M. Thus, compounds **2** and **3** promoted GLP-1 secretion independent of GPBAR1 and GPR119 receptors.

In order to understand the possible singling pathways involved in the GLP-1 secretion, different protein inhibitors, 2-APB (IP<sub>3</sub> inhibitor), KN-93 (Ca<sup>2+</sup>/CaMKII inhibitor), H89 (PKA inhibitor), GO6983 (PKC inhibitor) and PD98059 (MEK/ERK inhibitor), were tested in combination with **2** and **3** in STC-1 cells. As shown in Figure 5, the promoting effects of compounds **2** and **3** on GLP-1 secretion were obviously decreased when treated with different inhibitors. The GLP-1 promotion of **2** was significantly attenuated by 2-APB (42.3%), KN-93 (66.8%) and H89 (75.7%), but unresponsive to GO6983 and PD98059. As a comparison, the effect of compound **3** was reduced by KN-93 (61.0%), H89 (56.3%) and GO6983 (41.4%), but irrelevant to 2-APB and PD98059. Thus, both Ca<sup>2+</sup>/CaMKII and PKA pathways were closely involved in the GLP-1 promotion of compounds **2** and **3**.



**Figure 4.** The influence of **2** and **3** on cAMP concentration in GPBAR1 (A) and GPR119 (B) stably expressed CHO–K1 cells. LCA (lithocholic acid) and OEA (oleoylethanolamide) were used as positive controls. \*\*\*P<0.001 vs control. Data were expressed as mean  $\pm$  SDs (n= 3).

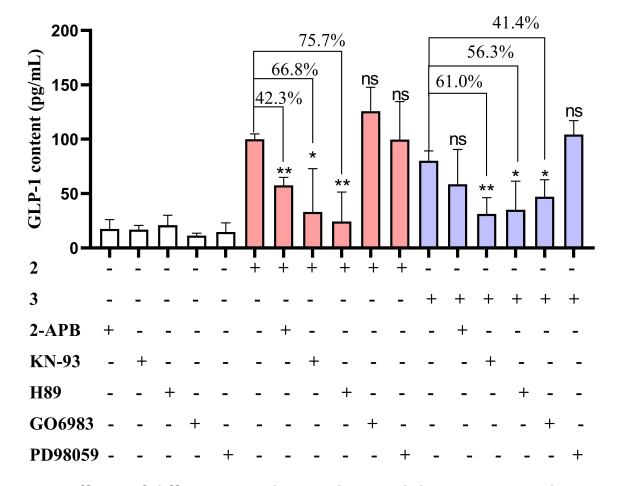


**Figure 5.** Effects of different signaling pathway inhibitors on **2**- and **3**-inducing GLP-1 secretion (40  $\mu$ M). Individual inhibitors were 2-APB (50  $\mu$ M), KN-93 (10  $\mu$ M), H89 (10  $\mu$ M), GO6983 (1  $\mu$ M) and PD98059 (25  $\mu$ M). \*P<0.05, \*\*P<0.01 vs compound-treated only group. Data were expressed as mean  $\pm$  SDs (n = 3).

## **DPP-4 Inhibition**

The endogenous GLP-1 was unstable and rapidly degraded by the DPP-4 enzyme *in vivo*. Therefore, all the isolates were further assayed for their inhibitory effects against DPP-4 enzyme (Table 3). Compound 1 exhibited a certain level of inhibition on DPP-4 with an IC<sub>50</sub> value of 311.0  $\mu$ M, whereas the half maximal inhibition of 2 and 3 was not reached at concentrations of 200 and 400  $\mu$ M. Thus, the increase of GLP-1 concentration in the supernatant of STC-1 cells might be partially due to the inhibition of DPP-4 activity.

#### **Molecular Docking**

In this study, compound 1 was revealed with DPP4 inhibitory activity. Thus, docking simulation was further conducted to investigate the interactions of 1 with DPP4 (2P8S), revealing a binding energy of -7.35 kcal/mol (Figure S1). The primary interactions were recognized as hydrogen bonds between the carbonyl group (C-15) of 1 and Arg61 residue, and hydrophobic effects of the aliphatic ring with Ile107 residue. Thus, the  $\alpha$ , $\beta$ -unsaturated  $\gamma$ -lactone may play a crucial role in maintaining DPP-4 inhibitory activity.

#### **Bioinformatics Study**

Considering that natural products always have multiple targets and mechanisms in exerting biological functions, network pharmacology analysis was further performed to predict the potential targets and pathways of 1 involved in the treatment of T2DM. As a result, 3472 human T2DM-related targets were collected from Disgenet, Genecards, OMIM and TTD databases (Table S1, Supporting Information) and 166 targets related to 1 were retrieved from PharMapper and SwissTargetPrediction databases (Table S2, Supporting Information). By comparing with Venny 2.1.0, a total of 80 overlapping proteins were recognized and selected for further functional analyses (Figure 6A). The overlapping proteins was analyzed by String and visualized by Cytoscape software to yield a core PPI network, comprising 13 nodes and 65 edges (Figure 6B). In the network, nodes represent proteins, while edges represent their interactions. Nodes with higher degrees are depicted with darker

Table 3. Inhibitor	e 3. Inhibitory activities of compounds 1–3 on DPP-4. [a]				
No.	Inhibition (%)		IC ( M)		
	400 μΜ	200 μΜ	IC <sub>50</sub> (μM)		
1	$66.7\pm16.5$	$20.7 \pm 2.9$	311.0		
2	$31.0\pm10.2$	$46.5\pm6.1$	/		
3	$41.3\pm4.5$	$39.9\pm8.0$	/		
Sitagliptin	/	/	0.05		

[a] Inhibition was denoted as mean  $\pm$  SDs (n = 3). Sitagliptin were used as the positive control.

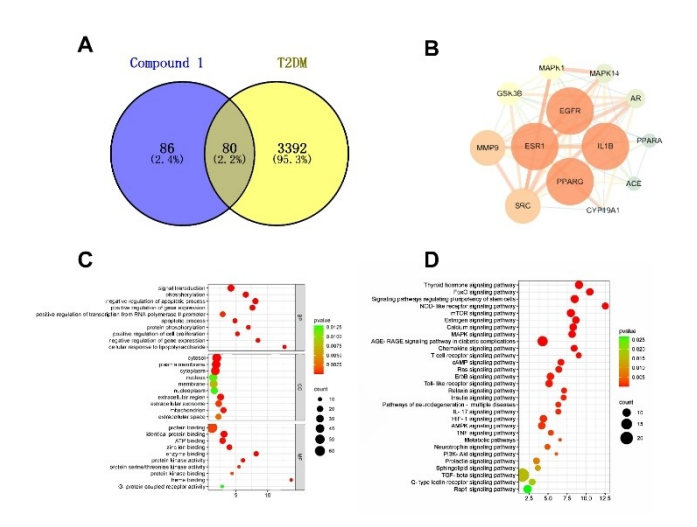


**Figure 6.** Bioinformatics analysis of 1 on T2DM. (A) Venn diagrams of identified targets; (B) PPI network of potential targets; (C) The bubble diagram of the top 10 significant terms from GO enrichment analysis, the abscissa representing the proportion of genes of interest, the ordinate representing each entry, the larger size of a dot indicating the larger number of genes annotated in the entry, the redder color of a dot standing for the lower *q* values; (D) Bubble diagram of the top 30 pathways from KEGG enrichment analysis, the abscissa representing the proportion of genes of interest and the ordinate representing each entry, the redder color meaning the lower *q* values.

colors and larger sizes, indicating they interact with more proteins, thus suggesting their roles are more significant within the network. Network topology analysis manifested the key targets of interleukin-1 beta (IL1B), epidermal growth factor receptor (EGFR), peroxisome proliferator activated receptor gamma (PPARG), estrogen receptor 1 (ESR1), steroid receptor coactivator (SRC) and matrix metalloproteinase 9 (MMP9). According to the previous study, IL-1B, EGFR and SRC played important roles in the pathological progression of diabetic kidney disease, [50-52] and PPARG and ESR1 enhanced GLUT expression to improve insulin sensitivity. [53,54] Thus, compound 1 might exert antidiabetic potency by ameliorating diabetic inflammation and insulin sensitivity.

GO analysis of the key targets generated 453 terms including 332 biological processes (BPs), 39 cellular components (CCs) and 83 molecular functions (MFs) (Table S3, Supporting Information), of which the top 10 statistically significant terms were visualized in a bubble diagram (Figure 6C). Compound 1 mainly acted in the biological processes of signal transduction, phosphorylation, regulation of gene expression and the molecular functions of protein binding, enzyme binding, and protein kinase activity. KEGG enrichment analysis yielded 133 related pathways (Table S4, Supporting Information), and the top 30 significant pathways with the highest gene counts were presented in Figure 6D, which showed high correlation with AGE-RAGE, Thyroid hormone, FoxO and NOD-like receptor pathways. Generally, AGE-RAGE and NOD-like receptor signaling pathways play important roles in oxidative stress and excessive inflammation, and the expression levels of RAGE and NOD2 are significantly increased in inflammation and diabetes.[55,56] Thus, compound 1 was expected to improve the oxidative stress by



blocking AGEs-RAGE and NOD-like receptor signaling pathways, thereby resisting the progression of diabetes. Meanwhile, compound 1 might ameliorate insulin resistance by activating thyroid hormone and FoxO signaling pathways. From the above evidence, compound 1 might have antidiabetic effects by improving inflammation, oxidative stress and insulin resistance via regulating diverse receptors and signaling pathways.

#### Conclusions

In this study, three unusual isospongian diterpenoids including a new one were isolated from the leaves of *A. tsao-ko* for the first time. Compound 1 showed inhibition on DPP-4 but without stimulative effects on GLP-1 secretion. Docking simulation demonstrated the importance of  $\gamma$ -lactone ring in maintaining activity. Compounds 2 and 3 were revealed with significant GLP-1 stimulation in STC-1 cells through Ca²+/CaMKII and PKA pathways, but irrelevant to GPBAR1 and GPR119 receptors. Moreover, bioinformatics study predicted that compound 1 exerted antidiabetic efficacy by improving inflammation, oxidative stress and insulin resistance. This study first revealed the presence of isospongian diterpenoids in *A. tsao-ko*, which have antidiabetic potency by promoting GLP-1 secretion and inhibiting GLP-1 degradation.

# **Experimental Section**

#### **General Experimental Procedures**

1D and 2D nuclear magnetic resonance (NMR) spectra were acquired on an Advance III-600 spectrometer (Bruker, Bremerhaven, Germany) with TMS as the internal standard. High-resolution mass spectra were detected on a Shimadzu LC/MS-IT-TOF mass spectrometer (Shimadzu, Kyoto, Japan). IR spectra were measured using a Bio-Rad FTS-135 spectrometer (Hercules, California, USA), and UV spectra were collected with a Shimadzu UV2401PC spectrophotometer (Shimadzu, Kyoto, Japan). Electronic circular dichroism (ECD) spectra were obtained using a circular dichroic spectrometer (Applied Photophysics, Surrey, UK). A Jasco P-1020 digital polarimeter (Horiba, Tokyo, Japan) was used to gain optical rotations. Column chromatography (CC) was performed on silica gel (200-300 mesh, Yantai Xinnuo, Yantai, China) and Sephadex LH-20 (GE Healthcare Bio-Sciences AB, Uppsala, Sweden). Thin-layer chromatography (TLC) analyses were conducted on silica gel GF254 plates (Yantai Xinnuo, Yantai, China). Medium pressure liquid chromatography (MPLC) separation was carried out using a QuikSep apparatus (Huideyi Technology, Beijing, China) with an Rp-C18 column. HPLC purification was performed on a Shimadzu LC-CBM-20 system (Shimadzu, Kyoto, Japan) with a ChromCore C8 column (5 μm, 9.4×250 mm).

#### **Plant Materials**

The leaves of *Amomum tsao-ko* Crevost et Lemaire were collected from Dushuyakou Village, Wenshan, Yunnan Province of China, in August 2018, which were authenticated by Dr. Jiang Zeng (Wenshan University). A voucher specimen (No. 201808At-2) was stored in the Key Laboratory of Phytochemistry and Natural

Medicines, Kunming Institute of Botany, Chinese Academy of Sciences.

#### **Extraction and Isolation**

The leaves of Amomum tsao-ko (10 kg) were powdered and extracted using aqueous EtOH (70%) at room temperature for two times. The combined EtOH was concentrated under reduced pressure and extracted by EtOAc. The EtOAc part was fractionated using silica gel column chromatography (Si CC) with an elution of acetone-petroleum ether (0:100-100:0) to yield ten fractions (Frs. 1-10). Fr. 8 (60.7 g) was loaded on a silica gel column and eluted with acetone-petroleum ether gradient (10:90-80:20) to produce six fractions, Fr. 8-1-8-6. Fr. 8-4 (5.1 g) was separated by a MCI CHP20P column using a MeOH-H<sub>2</sub>O system (20:80-100:0) to generate four fractions (Frs. 8-4-1-8-4-4). Fr. 8-4-1 (1.4 g) was fractionated using MPLC on an Rp-C18 column (MeOH-H2O, 10:90-70:30) to provide three sub-fractions, Fr. 8-4-1-1-8-4-1-3. Fr. 8-4-1-1 was purified by a Sephadex LH-20 column (MeOH) to give compound 1 (77 mg). Fr. 8-4-1-2 was purified by HPLC using a ChromCore C8 column (MeCN-H<sub>2</sub>O, 39:61, 3.0 mL/min) to generate compounds 2 (65 mg) and 3 (151 mg).

#### Spectroscopic Data

**Compound 2**: Colorless needles;  $C_{20}H_{28}O_4$ ;  $[\alpha]_D^{23}$  -175.2 (c 0.3, MeOH); UV (MeOH)  $\lambda_{\text{max}}$  (log  $\epsilon$ ): 217 (3.02) nm; IR (KBr)  $v_{\text{max}}$ : 3525, 2963, 2937, 1738, 1706, 1642, 1454, 1394, 1276, 1038, 988, 842 cm $^{-1}$ ; ECD (MeOH)  $\lambda_{\text{max}}$  ( $\Delta\epsilon$ ) 200 (7.63), 228 (-17.03) nm; HRESIMS m/z 355.1880 [M+Na] $^+$  (calcd. 355.1880, 0.0 mDa);  $^1$ H and  $^{13}$ C NMR data, see Table 1.

#### GLP-1 Secretion and DPP-4 Inhibition Assay

The assay for GLP-1 secretion<sup>[37]</sup> and DPP-4 inhibition<sup>[58]</sup> was performed according to the previous reports. 2-APB (IP<sub>3</sub> inhibitor), KN93 (Ca<sup>2+</sup>/CaMKII inhibitor), H89 (PKA inhibitor), GO6983 (PKC inhibitor) and PD98059 (MEK/ERK inhibitor) were used to test the signaling pathways involved in GLP-1 secretion. Cells were preincubated with inhibitors in KRB for 0.5 h before the treatment with compounds, and the supernatants were measured by GLP-1 ELISA Kits.

#### **GPBAR1 and GPR119 Agonistic Tests**

CHO–K1/GPBAR1 cells were cultured in Ham's F12 buffer supplemented with 10% FBS, 1% penicillin/streptomycin, and 200 µg/mL zeocin at 37 °C (5% CO<sub>2</sub>). CHO–K1/GPR119 cells were cultured in Ham's F12 K buffer supplemented with 10% TET-FBS, 1% penicillin/streptomycin, 100 µg/mL hygromycin, and 1 µg/mL doxycycline at 37 °C (5% CO<sub>2</sub>). After a 12-h incubation, cells were seeded in 384-well plates at a density of  $6\times10^5$  cells/mL, and treated with the tested compounds. Intracellular cAMP contents were measured using cAMP–Gs dynamic kits as reported previously.  $^{[59]}$ 

## **Statistical Analysis**

Statistical analysis was conducted using GraphPad Prism 8.0 software. Data were presented as mean  $\pm$  standard deviations (SDs). One-way ANOVA was used for multiple group comparisons, and pairwise comparisons were performed using independent t-tests. A p < 0.05 was considered statistically significant in all analyses.



## **Molecular Docking**

The 3D structure of 1 was obtained from the PubChem database, and the crystal structure of DPP-4 (PDB ID: 2P8S) was downloaded from the RCSB Protein Data Bank. AutoDock 4.2.6 was applied to simulate the interactions of ligand and protein. Results were visualized by PyMol software.

#### **Network Pharmacology Analysis**

The target genes of 1 were predicted via PharmMapper Server and SwissTargetPrediction database. T2DM related targets were retrieved from DisGeNET database, GeneCards database, OMIM and Therapeutic Target Database. To identify the possible targets, Venny 2.1.0 software was applied to obtain the intersection of target genes. The intersecting targets were submitted to the STRING database to create a protein–protein interaction (PPI) network. The gene ontology (GO) and Kyoto Encyclopedia of Genes and Genomes (KEGG) enrichment analyses were conducted using the functional annotation tool of DAVID database. [60]

#### **Author Contributions**

Yun Wang: Investigation, Writing – original draft. Sheng-Li Wu: Investigation, Writing – original draft. Xin-Yu Li: Investigation. Pianchou Gongpan: Methodology. Hang Fu: Methodology. Xiang-Ming Liao: Methodology. Yi Yang: Methodology. Mei Huang: Methodology. Yun-Bao Ma: Validation. Xiao-Yan Huang: Validation. Da-Hong Li: Supervision. Chang-An Geng: Conceptualization, Writing – review & editing, Supervision, Funding acquisition.

# **Acknowledgements**

This work was financially supported by the Yunnan Major Scientific and Technological Program (202202AE090035), the Yunnan Fundamental Research Projects (202201AV070010, 202301AS070069, 202402AA310003), Yunnan Province Science and Technology Department (202305AH340005), and the Fund of State Key Laboratory of Phytochemistry and Plant Resources in West China (P2022-KF12). We highly appreciate Dr. Jiang Zeng (Wenshan University) for the collection and authentication of the plant.

# **Conflict of Interests**

The authors declare no conflict of interest.

# Data Availability Statement

The data that support the findings of this study are available in the supplementary material of this article. **Keywords:** Amomum tsao-ko · Biological activity · GLP-1 secretion · Isospongian diterpenoids · Terpenoids

- [1] R. A. Keyzers, P. T. Northcote, M. T. Davies-Coleman, Nat. Prod. Rep. 2006, 23, 321–334.
- [2] M. A. Gonzalez, Curr. Bioact. Compd. 2007, 3, 1–36.
- [3] L. M. Frija, R. F. Frade, C. A. Afonso, Chem. Rev. 2011, 111, 4418–4452.
- [4] S. C. Bobzin, D. J. Faulkner, J. Org. Chem. 1989, 54, 3902-3907.
- [5] K. Gustafson, R. J. Andersen, H. Cun-heng, J. Clardy, *Tetrahedron Lett.* 1985, 26, 2521–2524.
- [6] M. Tischler, R. J. Andersen, M. I. Choudhary, J. Clardy, J. Org. Chem. 1991, 56, 42–47.
- [7] E. J. Dumdei, J. Kubanek, J. E. Coleman, J. Pika, R. J. Andersen, J. R. Steiner, J. Clardy, Can. J. Chem. 1997, 75, 773–789.
- [8] D. J. Faulkner, T. F. Molinski, R. J. Andersen, E. J. Dumdei, E. D. De Silva, Comp. Biochem. Phys. C-Comp. Pharm. 1990, 97, 233–240.
- [9] H. Yin, J.-G. Luo, L.-Y. Kong, J. Nat. Prod. 2013, 76, 237–242.
- [10] A. Faricha, P. Ahmadi, N. J. de Voogd, J. Tanaka, *Nat. Prod. Commun.* 2017, 12, 1011–1012.
- [11] T. Kodama, C. P. Wong, A. H. El-Desoky, H. H. W. Nyunt, H. Ngwe, I. Abe, H. Morita, *Fitoterapia* **2020**, *146*, 104705.
- [12] M. Ding, S. L. Wu, X. F. He, X. M. Zhang, C. A. Geng, Chin. J. Chin. Mater. Med. 2022, 47, 5849–5854.
- [13] M. R. Bhandari, N. Jong-Anurakkun, G. Hong, J. Kawabata, Food Chem. 2008, 106, 247–252.
- [14] T. Matsui, T. Tanaka, S. Tamura, A. Toshima, K. Tamaya, Y. Miyata, K. Tanaka, K. Matsumoto, *J. Agric. Food Chem.* **2007**, *55*, 99–105.
- [15] G. G. Adams, S. Imran, S. Wang, A. Mohammad, S. Kok, D. A. Gray, G. A. Channell, G. A. Morris, S. E. Harding, Food Res. Int. 2011, 44, 862–867.
- [16] International Diabetes Federation, IDF Diabetes Atlas, 10th ed., 2022.
- [17] E. Lalla, P. N. Papapanou, Nat. Rev. Endocrinol. 2011, 7, 738–748.
- [18] S. D. Prato, M. Matsuda, D. Simonson, L. Groop, P. Sheehan, F. Leonetti, R. Bonadonna, R. DeFronzo, *Diabetologia* 1997, 40, 687–697.
- [19] M. Brownlee, Nature 2001, 414, 813–820.
- [20] N. Kerru, A. Singh-Pillay, P. Awolade, P. Singh, Eur. J. Med. Chem. 2018, 152, 436–488.
- [21] X. Y. Xu, H. Y. Xu, Y. Shang, R. Zhu, X. X. Hong, Z. H. Song, Z. P. Yang, J. Pharm. Anal. 2021, 11, 398–404.
- [22] G. He, S. B. Yang, Y. Z. Wang, Arab. J. Chem. 2023, 16, 104936.
- [23] R. Cai, X. Yue, Y. Wang, Y. Yang, D. Sun, H. Li, L. Chen, J. Ethnopharmacol. 2021, 281, 114563.
- [24] S. Yang, Y. Xue, D. Chen, Z. Wang, Phytochem. Rev. 2022, 21, 1487– 1521.
- [25] S. S. Hong, J. H. Lee, Y. H. Choi, W. Jeong, E. K. Ahn, S. H. Lym, J. S. Oh, Tetrahedron Lett. 2015, 56, 6681–6684.
- [26] K. Y. Lee, S. H. Kim, S. H. Sung, Y. C. Kim, *Planta Med.* **2008**, *74*, 867–869.
- [27] X. Z. Yang, P. Küenzi, I. Plitzko, O. Potterat, M. Hamburger, *Planta Med.* 2009, 75, 543–546.
- [28] Q. S. Song, R. W. Teng, X. K. Liu, C. R. Yang, Chin. Chem. Lett. 2001, 12, 227–230.
- [29] J. G. Kim, H. Jang, T. P. L. Le, H. R. Hong, M. K. Lee, J. T. Hong, D. Lee, B. Y. Hwang, J. Nat. Prod. 2019, 82, 1886–1892.
- [30] T. T. Zhang, C. L. Lu, J. G. Jiang, J. Funct. Food. 2015, 18, 423–431.
- [31] G. He, S. B. Yang, Y. Z. Wang, *Arab. J. Chem.* **2023**, *16*, 104936.
- [32] T. T. Zhang, C. L. Lu, J. G. Jiang, Food Funct. 2014, 5, 1747–1754.
- [33] L. Q. Yu, N. Shirai, H. Suzuki, N. Sugane, T. Hosono, Y. Nakajima, M. Kajiwara, K. Takatori, J. Nutr. Sci. Vitaminol. 2010, 56, 171–176.
- [34] X. F. He, X. K. Zhang, C. A. Geng, J. Hu, X. M. Zhang, Y. Q. Guo, J. J. Chen, *Bioorg. Chem.* 2020, 96, 103638.
- [35] M. Ding, S. L. Wu, J. Hu, X. F. He, X. Y. Huang, T. Z. Li, Y. B. Ma, X. M. Zhang, C. A. Geng, *Phytochemistry* 2022, 199, 113204.
- [36] Q. Huang, Y. Pan, S. L. Wu, X. Y. Huang, J. Hu, Y. B. Ma, X. M. Zhang, C. A. Geng, *Phytochem. Lett.* **2022**, *48*, 87–93.
- [37] X. F. He, S. L. Wu, J. J. Chen, J. Hu, X. Y. Huang, T. Z. Li, X. M. Zhang, Y. Q. Guo, C. A. Geng, *Bioorg. Chem.* 2022, 120, 105653.
- [38] Z. T. Deng, J. J. Chen, C. A. Geng, *Bioorg. Chem.* **2020**, *95*, 103571.
- [39] C. Cui, S. L. Wu, J. J. Chen, P. Gongpan, M. Guan, C. A. Geng, J. Agric. Food Chem. 2023, 71, 16148–16159.
- [40] T. Wang, S. L. Wu, P. Liu, J. J. Chen, X. M. Zhang, C. A. Geng, Fitoterapia 2023, 167, 105502.
- [41] P. Liu, S. L. Wu, T. Wang, X. M. Zhang, C. A. Geng, *Phytochem. Lett.* 2023, 55, 75–79.
- [42] X. F. He, J. J. Chen, T. Z. Li, J. Hu, X. K. Zhang, Y. Q. Guo, X. M. Zhang, C. A. Geng, Chin. Chem. Lett. 2021, 32, 1202–1205.



- [43] X. F. He, J. J. Chen, X. Y. Huang, J. Hu, X. K. Zhang, Y. Q. Guo, X. M. Zhang, C. A. Geng, *Ind. Crop. Prod.* 2021, 160, 112908.
- [44] X. F. He, J. J. Chen, T. Z. Li, X. K. Zhang, Y. Q. Guo, X. M. Zhang, J. Hu, C. A. Geng, J. Agric. Food Chem. 2020, 68, 11434–11448.
- [45] X. F. He, H. M. Wang, C. A. Geng, J. Hu, X. M. Zhang, Y. Q. Guo, J. J. Chen, *Phytochemistry* 2020, 177, 112418.
- [46] M. L. Lund, G. Sorrentino, K. L. Egerod, C. Kroone, B. Mortensen, F. K. Knop, F. Reimann, F. M. Gribble, D. J. Drucker, E. J. P. de Koning, K. Schoonjans, F. Bäckhed, T. W. Schwartz, N. Petersen, *Diabetes* 2020, 69, 614–623
- [47] D. M. Lourenco, Clinics 2011, 66, 2183–2183.
- [48] S. H. Lee, H. M. Ko, W. Jee, H. Kim, W. S. Chung, H. J. Jang, Int. J. Mol. Sci. 2023, 24, 3682.
- [49] J. Park, K. S. Kim, K. H. Kim, I. S. Lee, H. S. Jeong, Y. Kim, H. J. Jang, Biochem. Biophys. Res. Commun. 2015, 468, 306–311.
- [50] R. C. Harris, Cells 2022, 11, 3416.
- [51] T. Zheng, H. Y. Wang, Y. Chen, X. Chen, Z. L. Wu, Q. Y. Hu, H. Sun, Front. Pharmacol. 2022, 13, 897046.
- [52] G. Li, J. Zhang, D. Liu, Q. Wei, H. Wang, Y. Lv, Z. Ye, G. Liu, L. Li, Front. Genet. 2021, 12, 767654.
- [53] H. I. Kim, Y. H. Ahn, Diabetes 2004, 53 (1), S60–S65.

- [54] R. S. Campello, A. B. Alves-Wagner, T. F. Lucas, R. C. Mori, D. T. Furuya, C. S. Porto, U. F. Machado, Curr. Top. Med. Chem. 2012, 12, 2059–2069.
- [55] C. Y. Shen, C. H. Lu, C. H. Wu, K. J. Li, Y. M. Kuo, S. C. Hsieh, C. L. Yu, Molecules 2020, 25, 5591.
- [56] P. Du, B. Fan, H. Han, J. Zhen, J. Shang, X. Wang, X. Li, W. Shi, W. Tang, C. Bao, Z. Wang, Y. Zhang, B. Zhang, X. Wei, F. Yi, Kidney Int. 2013, 84, 265–276.
- [57] Y. Yan, Z. Niu, C. Sun, P. Li, S. Shen, S. Liu, Y. Wu, C. Yun, T. Jiao, S. Jia, Y. Li, Z. Z. Fang, L. Zhao, J. Wang, C. Xie, C. Jiang, Y. Li, X. Feng, C. Hu, J. Jiang, H. Ying, *Nat. Commun.* 2022, *13*, 6408.
- [58] X. F. He, J. J. Chen, T. Z. Li, J. Hu, X. Y. Huang, X. M. Zhang, Y. Q. Guo, C. A. Geng, Chin. J. Chem. 2021, 39, 3051–3063.
- [59] A. M. Habib, P. Richards, G. J. Rogers, F. Reimann, F. M. Gribble, *Diabetologia* 2013, 56, 1413–1416.
- [60] B. T. Sherman, M. Hao, J. Qiu, X. L. Jiao, M. W. Baseler, H. C. Lane, T. Imamichi, W. Z. Chang, Nucl. Acids Res. 2022, 50, W216–W221.

Manuscript received: June 6, 2024 Accepted manuscript online: July 27, 2024 Version of record online: September 9, 2024